Received: 4 April 2019 | Revised: 20 June 2019 | Accepted: 21 June 2019

DOI: 10.1002/env.2596

RESEARCH ARTICLE

WILEY

Bayesian time-varying quantile regression to extremes

Fernando Ferraz Do Nascimento[1] | **Marcelo Bourguignon**[2]

[1]Departamento de Estatística, Universidade Federal do Piauí, Teresina, Brazil

[2]Departamento de Estatística, Universidade Federal do Rio Grande do Norte, Natal, Brazil

Correspondence
Marcelo Bourguignon, Departamento de Estatística, Universidade Federal do Rio Grande do Norte, Natal-RN 59078-970, Brazil.
Email: m.p.bourguignon@gmail.com

Abstract

Maximum analysis consists of modeling the maximums of a data set by considering a specific distribution. Extreme value theory (EVT) shows that, for a sufficiently large block size, the maxima distribution is approximated by the generalized extreme value (GEV) distribution. Under EVT, it is important to observe the high quantiles of the distribution. In this sense, quantile regression techniques fit the data analysis of maxima by using the GEV distribution. In this context, this work presents the quantile regression extension for the GEV distribution. In addition, a time-varying quantile regression model is presented, and the important properties of this approach are displayed. The parameter estimation of these new models is carried out under the Bayesian paradigm. The results of the temperature data and river quota application show the advantage of using this model, which allows us to estimate directly the quantiles as a function of the covariates. This shows which of them influences the occurrence of extreme temperature and the magnitude of this influence.

KEYWORDS

extreme value theory, generalized extreme value distribution, maximum analysis, quantile regression, time-varying models

1 | INTRODUCTION

Maxima analysis consists of collecting daily data over a long period, grouping them into maximums in blocks of size n and proposing a model for the analysis of these data. This type of analysis is one of the most important tools of extreme value theory (EVT), and it is useful for analyzing how often an event classified as "extreme" can occur.

The largest observation of a sample of the values $x_1, x_2, \ldots, x_n$ of a variable X is called the maximum and is denoted by $M_n = \max(x_1, x_2, \ldots, x_n)$. In a sample in which all the individuals are independently and identically distributed (i.i.d.), if we know the distribution of this variable, F_X, we may find the distribution of the maximum, which is given by $\Pr(M_n < y) = F_X(y)^n$. A problem in practice is that the distribution of the data F_X is often unknown or does not have a closed analytical form, making it difficult to model the maxima in these situations. The theorem of Fisher and Tippett (1928) presents an important result for the maximum and minimum boundary distributions. These authors show that, for any distribution F_X, the distribution of the maximums in blocks of size n, when $n \to \infty$, converges to one of the following three distributions: Gumbel, Fréchet, or Weibull.

Von Mises (1954) and Jenkinson (1955) propose the generalized extreme value (GEV) distribution, which encompasses the three limit distributions of Fisher and Tippett (1928), denoted by H, with the following distribution function:

$$H(y|\xi,\sigma,\mu) = \begin{cases} \exp\left\{-\left(1+\xi\left(\frac{(y-\mu)}{\sigma}\right)\right)^{-1/\xi}\right\}, & \text{if } \xi \neq 0, \\ \exp\left\{-\exp\left\{-\left(\frac{y-\mu}{\sigma}\right)\right\}\right\}, & \text{if } \xi = 0, \end{cases} \tag{1}$$

defined on the set $\{y : 1+\xi(y-\mu)/\sigma > 0\}$, where the parameter that satisfies $\mu \in \mathbb{R}$ is the location parameter, $\sigma > 0$ is the scale parameter, and $\xi \in \mathbb{R}$ is the shape parameter. Thus, for $\xi > 0$, the expression just given for the cumulative

distribution function is valid for $y > \mu - \sigma/\xi$, whereas for $\xi < 0$, it is valid for $y < \mu + \sigma/(-\xi)$. In the first case, at the lower end point, it equals 0; in the second case, at the upper end point, it equals 1. For $\xi = 0$, the expression just given for the cumulative distribution function is formally undefined and is replaced by the result obtained by taking the limit as $\xi \to 0$. The subfamilies of the distributions defined by $\xi = 0, \xi > 0$, and $\xi < 0$ correspond, respectively, to the Gumbel, Fréchet, and Weibull families of distributions.

Several approaches for the GEV distribution have already been proposed in the literature. Embrechts, Klüppelberg, and Mikosch (1997) and Coles (2001) present several parameter estimation techniques such as maximum likelihood and l-moments that can be applied using the package **evir** in R (Pfaff, Zivot, McNeil, & Stephenson, 2018). Gaetan and Grigoletto (2004) present a model with dynamically varying parameters. Nascimento and Silva (2016), through the package **MCMC4Extremes**, provide Bayesian inference for the GEV estimation in R.

A natural extension for maximum analysis is to observe how the presence of covariates can influence these measurements. In environmental data, elevation, latitude, and season have a strong influence on the measurements, and thus, it is necessary to add these factors into the model. In the context of extreme values, some studies have developed a regression model structure for the parameters of the generalized Pareto distribution (GPD) and GEV distribution. Cabras, Castellanos, and Gamerman (2011) consider adding seasonal covariates to the GPD parameter, applied to rain data. Nascimento, Gamerman, and Lopes (2011) model the exceedance of temperature considering altitude and latitude as covariates, describing a regression to its parameters.

Under EVT, it is important to observe the high quantiles of the distribution, which shows the probability of a risk event occurring in every t period. In this sense, quantile regression techniques fit the data analysis of maxima by using the GEV distribution. Despite the strong properties of the GEV distribution, its parameters do not correspond to the quantile, which complicates the interpretation of the regression models specified using this distribution. For the the GEV distribution, the quantile function can be obtained by inverting Equation (1), obtaining

$$q(p) = \begin{cases} \mu + \frac{\sigma}{\xi}\left[(-\log(p))^{-\xi} - 1\right], & \text{if } \xi \neq 0, \\ \mu - \sigma \log(-\log(p)), & \text{if } \xi = 0. \end{cases} \tag{2}$$

This quantile is a highly nonlinear function of the model parameters. In practice, the estimates of the quantiles can rarely be obtained directly. However, in some distributions, it is possible to obtain a reparametrization in terms of the quantiles and then insert a regression structure into these parameters, where it can be written as a function of the covariates. Nascimento, Gamerman, and Lopes (2016) obtain good results for their estimations of stock market returns at higher quantiles. Some quantile regressions have been carried out in a Bayesian context. Yu and Moyeed (2001) use the Metropolis–Hastings algorithm to estimate the parameters. Kozumi and Kobayashi (2011) show the case in which the sampling can be performed using Gibbs sampling. Gonçalves, Migon, and Bastos (2018) consider a dynamic linear model (DLM) in the quantile regression, where the parameters vary over time.

In this study, we propose a quantile linear regression model in which the response variable is a GEV distribution, adopting a new parametrization of this distribution indexed by using the quantile, scale, and shape parameters. In particular, in this work, the quantile regression quantifies the association of the explanatory variables with a quantile of a dependent variable. Furthermore, we propose a model for extreme values in which the reparametrized GEV distribution parameters are based on a dynamic quantile linear regression model in which the regression parameters vary over time. The main motivation for this new regression model is based on three issues as follows.

- The main advantage of our new parametrization and approach (quantile regression) is the straightforward interpretation of the regression coefficients in terms of the quantiles.
- The proposed model allows us to estimate the quantiles directly. None of the models cited above can estimate the quantiles directly (in the context of extreme values). Estimating the quantiles directly as a function of the covariates allows us to show which of them influences the occurrence of extreme temperature and the magnitude of this influence.
- The parameter estimation of these new models is carried out under the Bayesian paradigm. The Bayesian approach directly allows the use of the likelihood function, whereas other works (in the context of quantile regression) perform inference based on least squares estimators. They also use asymptotic properties to find the distribution of the parameters, whereas the posterior distribution is precise.

With these contributions above, we provide a complete tool for modeling extreme values based on our quantile regression of the GEV distribution.

The remainder of the paper is organized as follows. Section 2 describes the model of the quantile regression of the GEV distribution and extends it to a dynamic regression. The details of the Bayesian inference and MCMC algorithm are also presented. Section 3 shows simulations of the proposed model, highlighting the efficiency of the inference procedure in capturing the true values of the parameters. Section 4 applies temperature and river quota data in the United States and Brazil to the proposed model. Section 5 concludes.

2 | THE PROPOSED MODELS

Quantile regression models are typically constructed to model the median of a distribution. Despite the strong properties of the GEV distribution, its location, scale, and shape parameters do not correspond to the p-quantile, which complicates the interpretation of quantile regression models specified using this distribution. In this context, we consider a new parametrization of the GEV distribution in terms of the p-quantile parameter in this section.

Let $Z_1, \ldots, Z_m$ be i.i.d. with a given distribution function F. Let $Y_1, \ldots, Y_n$, the maximum observations of the vector X in blocks of size l, be sufficiently large. EVT states that the maximum can be approximated by the GEV distribution, denoting $Y_i \sim \text{GEV}(\mu, \sigma, \xi)$, whose probability distribution function is given by (1). By considering the quantile p of the GEV distribution given by (2), we can also reparametrize the GEV distribution as a function of the p-quantile. From the function of the quantile, we find that the most parsimonious way of conducting the reparametrization is using the location parameter μ, where we can then write, for the general case $\xi \neq 0$,

$$\mu = q(p) - \frac{\sigma}{\xi}[(-\log(p))^{-\xi} - 1]. \tag{3}$$

This parametrization has not been proposed in the statistical literature. Hence, we can rewrite the GEV distribution according to the parameters $q(p), \sigma$, and ξ, whose cumulative distribution function is now given by

$$H(y|q(p), \sigma, \xi) = \exp\left\{-\left[(-\log(p))^{-\xi} + \xi\left(\frac{y - q(p)}{\sigma}\right)\right]^{-1/\xi}\right\}, \tag{4}$$

where the quantile $p \in (0, 1)$ is assumed to be known. Hereafter, we use the notation $Y \sim \text{GEV}(q(p), \sigma, \xi)$ to indicate that Y is a random variable following a GEV distribution with quantile parameter $q(p)$, scale parameter σ, and shape parameter ξ.

2.1 | Quantile regression for the GEV model

The main motivation of using the quantile regression model is to write the quantile as a function of the covariates to allow us to interpret which factors influence the high quantiles. In this subsection, the proposed model is composed by adding the regression models into the three parameters $(q(p), \sigma, \xi)$ of the distribution, using a similar approach to Nascimento et al. (2011) for the GPD.

Let $Y_1, \ldots, Y_n$ be the n independent random variables, where each $Y_i, i = 1, \ldots, n$, follows the GEV distribution with quantile parameter $q(p)$, scale parameter σ, and shape parameter ξ. Suppose the $q(p)$, σ, and ξ parameters of Y_i satisfy the following functional relations:

$$g_1(q(p)_i) = \mathbf{x}_i^\top \boldsymbol{\beta}_p, \quad g_2(\sigma_i) = \mathbf{z}_i^\top \boldsymbol{\nu} \quad \text{and} \quad g_3(\xi_i) = \mathbf{w}_i^\top \boldsymbol{\alpha}, \tag{5}$$

where $\boldsymbol{\beta}_p = (\beta_{p,1}, \ldots, \beta_{p,k})^\top$, $\boldsymbol{\nu} = (\nu_1, \ldots, \nu_l)^\top$, and $\boldsymbol{\alpha} = (\alpha_1, \ldots, \alpha_m)^\top$ are the vectors of the unknown regression coefficients, which are assumed to be functionally independent; $\boldsymbol{\beta}_p \in \mathbb{R}^k$, $\boldsymbol{\nu} \in \mathbb{R}^l$, and $\boldsymbol{\alpha} \in \mathbb{R}^m$, with $k + l + m < n$; and $\mathbf{x}_i = (x_{i,1}, \ldots, x_{i,k})^\top$, $\mathbf{z}_i = (z_{i,1}, \ldots, z_{i,l})^\top$, and $\mathbf{w}_i = (w_{i,1}, \ldots, w_{i,m})^\top$ are the observations of the k, l, and m known regressors, for $i = 1, \ldots, n$. Furthermore, we assume that the covariate matrices $\mathbf{X} = (\mathbf{x}_1, \ldots, \mathbf{x}_n)^\top$, $\mathbf{Z} = (\mathbf{z}_1, \ldots, \mathbf{z}_n)^\top$, and $\mathbf{W} = (\mathbf{w}_1, \ldots, \mathbf{w}_n)^\top$ have the rank k, l, and m, respectively. The link functions $g_1 : \mathbb{R} \to \mathbb{R}$, $g_2 : \mathbb{R}^+ \to \mathbb{R}$, and $g_3 : \mathbb{R}^+ \to \mathbb{R}$ in (5) must be strictly monotone, positive, and at least twice differentiable, such that $q(p)_i = g_1^{-1}(\mathbf{x}_i^\top \boldsymbol{\beta}_p)$, $\sigma_i = g_2^{-1}(\mathbf{z}_i^\top \boldsymbol{\nu})$, and $\xi_i = g_3^{-1}(\mathbf{w}_i^\top \boldsymbol{\alpha})$, with $g_1^{-1}(\cdot)$, $g_2^{-1}(\cdot)$, and $g_3^{-1}(\cdot)$ being the inverse functions of $g_1(\cdot)$, $g_2(\cdot)$, and $g_3(\cdot)$, respectively.

Based on the parametric space of the GEV written in the form in (4), we consider here the following link functions:

$$q(p)_i = \mathbf{x}_i^\top \boldsymbol{\beta}_p, \quad \sigma_i = \exp\left(\mathbf{z}_i^\top \boldsymbol{\nu}\right) \quad \text{and} \quad \xi_i = \exp\left(\mathbf{w}_i^\top \boldsymbol{\alpha}\right) - 1. \tag{6}$$

Proposition 1. *Let $q(p)$ be the p-quantile of the GEV distribution written in the function of the covariates as (5). Let $q(p^*)$ be a quantile from the same distribution, for a $p^* \neq p$. Then, the angular coefficients $\beta_{j,p} = \beta_{j,p^*}$, for $j = 1, \ldots, k$, and*

$$\beta_{0,p^*} = \beta_{0,p} + \frac{\sigma}{\xi}\left[(-\log(p^*))^{-\xi} - (-\log(p))^{-\xi}\right].$$

Proof. We saw in (2) that a p-quantile can be written as

$$q(p^*) = \mu + \frac{\sigma}{\xi}\left[(-\log(p^*))^{-\xi} - 1\right].$$

The proof consists of writing μ in the function of $q(p)$ as in (3):

$$\begin{aligned} q(p^*) &= q(p) - \frac{\sigma}{\xi}[(-\log(p))^{-\xi} - 1] + \frac{\sigma}{\xi}\left[(-\log(p^*))^{-\xi} - 1\right] \\ &= q(p) + \frac{\sigma}{\xi}\left[(-\log(p^*))^{-\xi} - (-\log(p))^{-\xi}\right]. \end{aligned}$$

Thus, by writing $q(p)$ as in (5), we have

$$\begin{aligned} q(p^*)_i &= \beta_{p,0} + \beta_{p,1}x_{1,i} + \ldots + \beta_{p,k}x_{k,i} + \frac{\sigma}{\xi}\left[(-\log(p^*))^{-\xi} - (-\log(p))^{-\xi}\right] \\ &= \underbrace{\beta_{0,p} + \frac{\sigma}{\xi}\left[(-\log(p^*))^{-\xi} - (-\log(p))^{-\xi}\right]}_{\beta_{p^*,0}} + \beta_{p,1}x_{1,i} + \ldots + \beta_{p,k}x_{k,i}. \end{aligned}$$

Considering a sample $Y_1, \ldots, Y_n$ with a GEV distribution function as in (4), with the parameters given as in (6), the likelihood function is given by

$$L(y;\Theta) = \prod_{i=1}^{n} h(y_i; q(p)_i, \sigma_i, \xi_i), \tag{7}$$

where the parameter vector is given by $\Theta = (\boldsymbol{\beta_p}, \boldsymbol{\nu}, \boldsymbol{\alpha})$ and h is the GEV density of (4). In this paper, the parameter estimation of this new model was carried out under the Bayesian paradigm. The Bayesian approach allows us to use the likelihood function, whereas other works perform their inference based on classic inference techniques. They use asymptotic properties to find the distribution of the parameters, whereas the posterior distribution is precise. The priors of the regression coefficients are chosen to be normal with a large variance for $\boldsymbol{\beta_p}$, $\boldsymbol{\nu}$, and $\boldsymbol{\alpha}$, and are given by

$$\beta_{p,0} \sim \mathrm{N}(a_{p,0}, V_\beta), \quad \beta_{p,i} \sim \mathrm{N}(0, V_\beta), i = 1, \ldots, k,$$

$$\nu_i \sim \mathrm{N}(0, V_\nu), i = 0, \ldots, l, \quad \alpha_i \sim \mathrm{N}(0, V_\alpha), i = 0, \ldots, l.$$

Nascimento et al. (2011) show that, for the GPD, these prior densities work well in both simulations and environmental data applications. By joining the likelihood with the prior, we obtain the posterior distribution. The posterior density can be written, in log form, as

$$\begin{aligned} \pi(\Theta|y) = &\sum_{i=1}^{n} \log[h(y_i; q(p)_i, \sigma_i, \xi_i)] + \frac{(\beta_{p,0} - a_{p,0})^2}{2V_\beta} - \sum_{i=1}^{k}\left(\frac{\beta_{p,i}^2}{2V_\beta}\right) \\ &- \sum_{i=0}^{l}\left(\frac{\nu_i^2}{2V_\nu}\right) - \sum_{i=0}^{m}\left(\frac{\alpha_i^2}{2V_\alpha}\right). \end{aligned}$$

MCMC techniques (Gamerman & Lopes, 2006) of the sampling points of the parametric vector were performed. As any specific parameter provides a known full conditional distribution, the Metropolis–Hastings algorithm was used for all the parameters. The vectors $\boldsymbol{\beta_p}$, $\boldsymbol{\nu}$, and $\boldsymbol{\alpha}$ were sampled in the Metropolis blocks procedure. □

2.2 | A dynamic quantile regression for the GEV model

In many situations, data behavior may vary over time. Time series analysis (Prado & West, 2010) can model data that vary as time passes. Under the Bayesian approach, West and Harrison (1997) capture the time variation by using the DLM. Gonçalves et al. (2018) present a quantile regression model using the DLM applied to an asymmetric Laplace distribution.

In the EVT context, Huerta and Sansó (2007) use the first-order dynamic model for the location parameter μ of the GEV distribution. Nascimento, Gamerman, and Lopes (2016) display the DLM for the shape and scale parameters of the GPD. Lima, Nascimento, and Ferraz (2018) extend this idea, considering a dynamic regression model for the GPD parameters.

In this section, we propose a model in which the GEV parameters in (4) vary according to the dynamic regression model; that is, temporal dependence is induced by allowing the GEV parameters to vary over time. The general structure of this model, which can be seen, for example, in West and Harrison (1997), is given by

$$\begin{pmatrix} \xi_t \\ \sigma_t \\ q(p)_t \end{pmatrix} = F_t^{\top}\beta_t + \lambda_t \quad \text{and} \quad \beta_t = g_t\beta_{t-1} + \omega_t,$$

where, in a dynamic regression model with s covariates, $F_t^{\top} = (1, x_{1t}, x_{2t}, \ldots, x_{st})$, $\boldsymbol{\beta}_t^{\top} = (1, \beta_{0t}, \beta_{1t}, \ldots, \beta_{st})$, G_t is an identity matrix $k \times k$, and $\omega_t = (1, \omega_{0t}, \omega_{1t}, \ldots, \omega_{st})$.

Considering the GEV parameters, we can propose the following model structure:

$$\begin{aligned}
\ell\xi_t &= \boldsymbol{\beta}_{\xi,t} + \lambda_{\xi,t}, \quad \lambda_{\xi,t} \sim \mathrm{N}(0, 1/V_\xi),\\
\boldsymbol{\beta}_{\xi,t,k} &= \beta_{\xi,t-1,k} + \omega_{\xi,t}, \quad \omega_{\xi,t} \sim \mathrm{N}(0, 1/W_\xi),\\
\ell\sigma_t &= \boldsymbol{\beta}_{\sigma,t} + \lambda_{\sigma,t}, \quad \lambda_{\sigma,t} \sim \mathrm{N}(0, 1/V_\sigma),\\
\beta_{\sigma,t,k} &= \beta_{\sigma,t-1,k} + \omega_{\sigma,t}, \quad \omega_{\sigma,t} \sim \mathrm{N}(0, 1/W_\sigma),\\
q(p)_t &= \boldsymbol{\beta}_{p,t} + \lambda_{p,t}, \quad \lambda_{p,t} \sim \mathrm{N}(0, 1/V_p),\\
\beta_{p,t,k} &= \beta_{p,t-1,k} + \omega_{p,t}, \quad \omega_{p,t} \sim \mathrm{N}(0, 1/W_p),
\end{aligned} \tag{8}$$

where $\ell\xi_t = \log(\xi_t + 1)$, $\boldsymbol{\beta}_{\xi,t} = \sum_{k=0}^{l} \beta_{\xi,t,k}X_{t,k}$, $\ell\sigma_t = \log(\sigma_t)$, $\boldsymbol{\beta}_{\sigma,t} = \sum_{k=0}^{p} \beta_{\sigma,t,k}X_{t,k}$, $\boldsymbol{\beta}_{p,t} = \sum_{k=0}^{m} \beta_{p,t,k}X_{t,k}$, and $\theta_{\xi,t}$, $\theta_{\sigma,t}$, $\theta_{p,t}$, $t = 0, \ldots, T$, $V_\xi, W_\xi, V_\sigma, W_\sigma, V_p, W_p$ are the model hyperparameters. Usually, these hyperparameters are choosing such that provide low variability in successive points in time, as in environmental data the changes are smooth, as cited as an example in (Lima et al., 2018). Usually these precision parameters are high and usually chosen between 1,000 and 10,000.

Combining the likelihood function in (7) with the prior distribution structure given in (8), we find that the parameters of the dynamic structure of the model have a known closed form and can be estimated by using Gibbs sampling. The following distributions are thus obtained as

$$\begin{aligned}
V_\xi &\sim \mathrm{Gamma}\left(\frac{T}{2} + f_\xi; \frac{1}{2}\sum_{t=1}^{T}(\ell\xi_t - \boldsymbol{\beta}_{\xi,t})^2 + o_\xi\right),\\
W_{\xi,k} &\sim \mathrm{Gamma}\left(\frac{T}{2} + \ell_\xi; \frac{1}{2}\sum_{t=1}^{T}(\beta_{\xi,t,k} - \beta_{\xi,t-1,k})^2 + m_\xi\right),\\
\beta_{\xi,0,k} &\sim \mathrm{N}\left(\frac{m_0/C_0 + W_{\xi,k}\beta_{\xi,1,k}}{1/C_0 + W_{\xi,k}}; \frac{1}{\frac{1}{C_0} + W_{\xi,k}}\right),\\
\beta_{\xi,t,k} &\sim \mathrm{N}\left(\frac{W_{\xi,k}\beta_{\xi,t-1,k} + W_{\xi,k}\beta_{\xi,t+1,k} + V_\xi S_{t,k}X_{t,k}}{2W_{\xi,k} + V_\xi X_{t,k}^2}; \frac{1}{2W_{\xi,k} + V_\xi X_{t,k}^2}\right), \quad t = 1, \ldots, T-1
\end{aligned}$$

$$\beta_{\xi,T,k} \sim \mathrm{N}\left(\frac{W_{\xi,k}\beta_{\xi,T-1,k} + V_\xi S_{T,k} X_{T,k}}{W_{\xi,k} + V_\xi X_{T,k}^2}; \frac{1}{W_{\xi,k} + V_\xi X_{t,k}^2}\right),$$

$$V_\sigma \sim \mathrm{Gamma}\left(\frac{T}{2} + f_\sigma; \frac{1}{2}\sum_{t=1}^{T}(\ell\sigma_t - \boldsymbol{\beta}_{\sigma,t})^2 + o_\sigma\right),$$

$$W_{\sigma,k} \sim \mathrm{Gamma}\left(\frac{T}{2} + \ell_\sigma; \frac{1}{2}\sum_{t=1}^{T}(\beta_{\sigma,t,k} - \beta_{\sigma,t-1,k})^2 + m_\sigma\right),$$

$$\beta_{\sigma,0,k} \sim \mathrm{N}\left(\frac{m_0/C_0 + W_{\sigma,k}\beta_{\sigma,1,k}}{1/C_0 + W_{\sigma,k}}; \frac{1}{\frac{1}{C_0} + W_{\sigma,k}}\right),$$

$$\beta_{\sigma,t,k} \sim \mathrm{N}\left(\frac{W_{\sigma,k}\beta_{\sigma,t-1,k} + W_{\sigma,k}\beta_{\sigma,t+1,k} + V_\sigma S_{t,k} X_{t,k}}{2W_{\sigma,k} + V_\sigma X_{t,k}^2}; \frac{1}{2W_{\sigma,k} + V_\sigma X_{t,k}^2}\right), \quad t = 1, \ldots, T-1$$

$$\beta_{\sigma,T,k} \sim \mathrm{N}\left(\frac{W_{\sigma,k}\beta_{\sigma,T-1,k} + V_\sigma S_{T,k} X_{T,k}}{W_{\sigma,k} + V_\sigma X_{T,k}^2}; \frac{1}{W_{\sigma,k} + V_\sigma X_{t,k}^2}\right),$$

$$V_p \sim \mathrm{Gamma}\left(\frac{T}{2} + f_p; \frac{1}{2}\sum_{t=1}^{T}(q(p)_t - \boldsymbol{\beta}_{p,t})^2 + o_p\right),$$

$$W_{p,k} \sim \mathrm{Gamma}\left(\frac{T}{2} + \ell_p; \frac{1}{2}\sum_{t=1}^{T}(\beta_{p,t,k} - \beta_{p,t-1,k})^2 + m_p\right),$$

$$\beta_{p,0,k} \sim \mathrm{N}\left(\frac{m_0/C_0 + W_{p,k}\beta_{p,1,k}}{1/C_0 + W_{p,k}}; \frac{1}{\frac{1}{C_0} + W_{p,k}}\right),$$

$$\beta_{p,t,k} \sim \mathrm{N}\left(\frac{W_{p,k}\beta_{p,t-1,k} + W_{p,k}\beta_{p,t+1,k} + V_p S_{t,k} X_{t,k}}{2W_{p,k} + V_p X_{t,k}^2}; \frac{1}{2W_{p,k} + V_p X_{t,k}^2}\right), \quad t = 1, \ldots, T-1$$

$$\beta_{p,T,k} \sim \mathrm{N}\left(\frac{W_{p,k}\beta_{p,T-1,k} + V_p S_{T,k} X_{T,k}}{W_{p,k} + V_p X_{T,k}^2}; \frac{1}{W_{p,k} + V_p X_{t,k}^2}\right).$$

3 | SIMULATION STUDY

To study the behavior of the quantile regression model for the GEV distribution, the proposed model was simulated. We consider simulations of the model (2.1) with the sample sizes $n = 400, 1000, 2000, 5000$ and quantile regression in $p = (0.80, 0.95, 0.99)$, which under EVT represents the return level expected once every $t = (5, 20, 100)$ periods. The simulation was performed in the following steps. We first simulated two covariates. The first covariate was given by $x_{1,t} = \cos(2\pi/12)$, simulating a seasonal effect. The second covariate was given by $x_{2,t} \sim \mathrm{N}(0, 1)$. Second, we assigned parameters to these variables. We considered $\boldsymbol{\beta}_p = (300, 2, -2)$, $\boldsymbol{\nu} = (2, -0.1, 0.2)$, and $\boldsymbol{\beta}_\xi = (-0.2, -0.1, 0.3)$. Third, through the link functions given in (6), we assigned the values $(q(p)_i, \sigma_i,$ and $\xi_i)$. Finally, we generated $Y_i \sim \mathrm{GEV}(q(p)_i, \sigma_i, \xi_i)$.

Table 1 shows the estimates of the parameters for the different quantiles and sample sizes. In most configurations, the true value of the parameter is within the credibility interval. For larger sample sizes, we observe more accurately with shorter credibility intervals. The main estimation difficulties occur for the parametrization involving the 99% quantile

TABLE 1 Simulations: summary of the estimation results for the proposed model

			$n = 400$	
	T	p=0.80	p=0.95	p=0.99
$\beta_{p,0}$	300	299.2 (298.2; 300.3)	300.5 (299.0; 301.9)	299.9 (298.4; 301.4)
$\beta_{p,1}$	2	1.61 (0.62; 2.73)	2.71 (1.49; 3.88)	1.99 (0.75; 3.31)
$\beta_{p,2}$	−2	−2.25 (−3.19; −1.50)	−1.94 (−3.14; −0.87)	−2.02 (−2.90; −1.20)
ν_0	2	1.94 (1.86;2.02)	2.01 (1.93;2.09)	1.94 (1.87;2.03)
ν_1	−0.1	−0.11 (−0.20; −0.02)	−0.06 (−0.16; 0.04)	−0.07 (−0.12; 0.00)
ν_2	0.2	0.20 (0.13; 0.27)	0.20 (0.14; 0.26)	0.18 (0.13; 0.23)
α_0	−0.2	−0.14 (−0.22; −0.06)	−0.20 (−0.27; −0.12)	−0.16 (−0.21; −0.12)
α_1	−0.1	−0.03 (−0.11; 0.06)	−0.12 (−0.17; −0.06)	−0.10 (−0.11; −0.09)
α_2	0.3	0.27 (0.21; 0.34)	0.30 (0.27; 0.33)	0.29 (0.28; 0.30)
			n=1,000	
	T	p=0.80	p=0.95	p=0.99
$\beta_{p,0}$	300	299.7 (299.1; 300.4)	300.6 (299.8; 301.7)	300.5 (299.5; 301.5)
$\beta_{p,1}$	2	2.00 (1.43; 2.64)	1.72 (0.98; 2.34)	2.46 (1.72; 3.17)
$\beta_{p,2}$	−2	−2.41 (−2.87; −1.93)	−1.77 (−2.38; −1.14)	−1.63 (−2.18; −1.04)
ν_0	2	1.96 (1.92; 2.01)	1.97 (1.93; 2.03)	2.04 (1.99; 2.07)
ν_1	−0.1	−0.09 (−0.14; −0.03)	−0.08 (−0.14; −0.03)	−0.09 (−0.13; −0.05)
ν_2	0.2	0.22 (0.18; 0.26)	0.19 (0.16; 0.22)	0.19 (0.17; 0.23)
α_0	−0.2	−0.20 (−0.24; −0.15)	−0.16 (−0.20; −0.12)	−0.20 (−0.23; −0.18)
α_1	−0.1	−0.10 (−0.17; −0.04)	−0.10 (−0.12; −0.08)	−0.10 (−0.11; −0.09)
α_2	0.3	0.30 (0.24; 0.33)	0.29 (0.28; 0.31)	0.30 (0.29; 0.31)
			n=2,000	
	T	p=0.80	p=0.95	p=0.99
$\beta_{p,0}$	300	299.9 (299.4; 300.3)	300.0 (299.3; 300.6)	299.8 (299.1; 300.6)
$\beta_{p,1}$	2	2.13 (1.70; 2.56)	1.98 (1.51; 2.41)	2.15 (1.71; 2.60)
$\beta_{p,2}$	−2	−2.05 (−2.37; −1.77)	−2.00 (−2.38; −1.64)	−2.05 (−2.33; −1.71)
ν_0	2	1.98 (1.94; 2.01)	2.00 (1.97; 2.04)	2.01 (1.98; 2.05)
ν_1	−0.1	−0.08 (−0.12; −0.04)	−0.12 (−0.16; −0.09)	−0.10 (−0.12; −0.08)
ν_2	0.2	0.20 (0.17; 0.22)	0.20 (0.18; 0.21)	0.21 (0.19; 0.23)
α_0	−0.2	−0.17 (−0.21; −0.14)	−0.21 (−0.24; −0.18)	−0.21 (−0.24; −0.19)
α_1	−0.1	−0.09 (−0.13; −0.24)	−0.09 (−0.10; −0.08)	−0.10 (−0.11; −0.10)
α_2	0.3	0.28 (0.26; 0.31)	0.30 (0.29; 0.31)	0.30 (0.29; 0.31)
			n=5,000	
	T	p=0.80	p=0.95	p=0.99
$\beta_{p,0}$	300	300.1 (299.8; 300.4)	299.8 (299.4; 300.1)	299.7 (299.3; 300.2)
$\beta_{p,1}$	2	1.90 (1.65; 2.19)	2.09 (1.80; 2.40)	2.05 (1.75; 2.35)
$\beta_{p,2}$	−2	−1.92 (−2.10; −1.76)	−2.14 (−2.34; −1.97)	−2.15 (−2.34; −1.93)
ν_0	2	1.97 (1.96; 2.01)	1.98 (1.96; 2.00)	1.97 (1.96; 1.97)
ν_1	−0.1	−0.08 (−0.11; −0.05)	−0.11 (−0.13; −0.08)	−0.12 (−0.11; −0.09)
ν_2	0.2	0.19 (0.17; 0.20)	0.20 (0.19; 0.22)	0.20 (0.19; 0.31)
α_0	−0.2	−0.18 (−0.20; −0.16)	−0.20 (−0.22; −0.18)	−0.19 (−0.20; −0.19)
α_1	−0.1	−0.10 (−0.12; −0.08)	−0.10 (−0.11; −0.09)	−0.10 (−0.10; −0.09)
α_2	0.3	0.30 (0.29; 0.31)	0.30 (0.29; 0.31)	0.30 (0.29; 0.30)

Note. Posterior means, with 95% credibility intervals, are in parentheses.

with $n = 5,000$, where a too-slow standard deviance of the parameter estimations results in some cases where the true value is in the limit of 95% credibility interval (CI).

Figure 1 shows the true $q(0.95)$ over time, with their respective credibility interval. The left part of the figure shows that, for the series of $n = 400$ observations, the difference between the true quantiles and their estimates is practically imperceptible. The right part of the figure, where this same graph is enlarged for a small part of the series, shows that the true series are all within the estimated credibility intervals.

Figure 2 shows the true and estimated $q(0.99)$ over time ($n = 5000$). Although we find no difference when plotting the whole data series, by enlarging the figure to show a shorter series, we realize that the credibility interval for larger samples is much shorter than in the previous case and that the estimated values are closer to the true values than the first simulation. In all of the 5,000 points, the true 99% quantile is inside the credibility interval of estimated quantile.

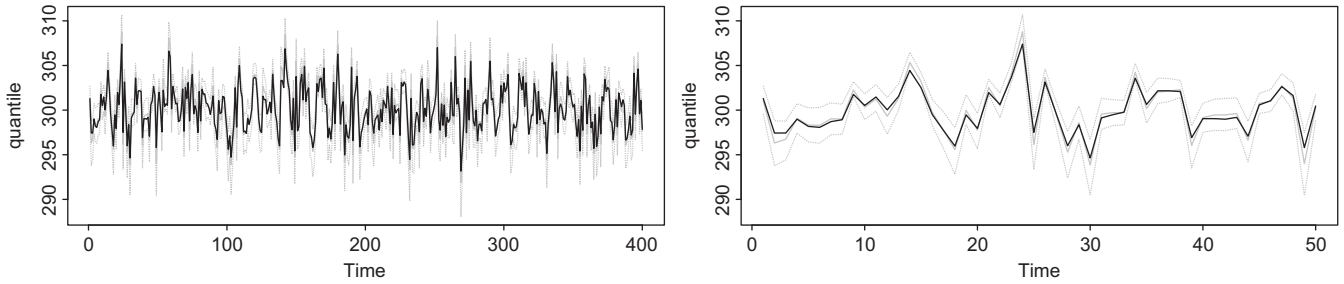

FIGURE 1 Simulations for $n = 400$: True quantile (black line), with posterior mean (grey line) and 95% CI (grey dots). (Left) Full observations. (Right) Zoom in first 50 observations

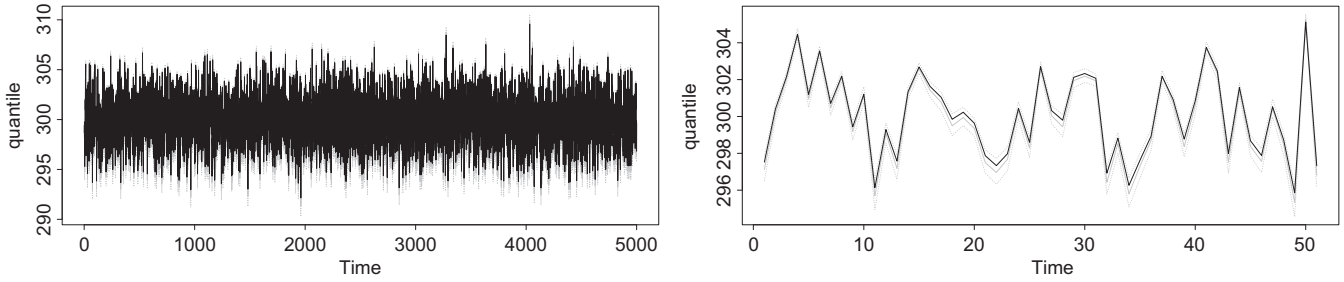

FIGURE 2 Simulations for $n = 5000$: True quantile (black line), with posterior mean (grey line) and 99% CI (grey dots). (Left) Full observations. (Right) Zoom in 50 observations

In order to verify the quality of the simulation method, 100 replications were simulated for each configuration of n and p. For each replication, we calculated the posterior mean of the parameters. We obtained the Average os 100 posterior means (APM), the average of the mean standard error (AMSE), and the proportion of replicates where the true value of parameter is inside the 95% credibility interval (CPI). These results are presented in Table 2. In all cases, APM is very close than the true value of the parameter. In addition, CPI is around the desired value of 0.95 in almost all cases, except the case where $n = 5000$ and $p = 0.99$. In this specific case, the low width of CI seen in Table 2 that indicates a small difference of posterior mean from the true value can be sufficient to the true value outside the 95% CI. Although the estimates of parameters should not be inside the 95% CI, Figure 2 shows that the resulting quantile of linear combination of parameters and covariates are inside the 95% CI.

4 | APPLICATIONS TO ENVIRONMENTAL MODELING

In this section, we apply the methodology considered in Section 2 to three real data sets. The proposed models are used to study two temperature data sets, namely, maxima in the United States and maxima in the state of Piauí in Brazil (quantile regression model), and applied to examine the monthly maxima quota of Gurgueia River in the state of Piauí (quantile dynamic model). The required numerical evaluations for the data analysis were carried out by using the R software.

4.1 | Annual maximum temperature in the United States

In the first application, we consider a data set consisting of the maxima annual temperature in 84 cities in the contiguous United States. The data are in degrees Fahrenheit, and we have available observations from 1995 to 2008. We consider standardized latitude and elevation as the covariates. Lower temperatures are usually expected at higher latitude and elevation.

For the three GEV parameters, we use the covariate vector $x = (x_0, x_1, x_2, x_3)$, where $x_0 = 1$ represents the intercept, $x_1 = (l - \bar{l})/\sigma_l$, $x_2 = (e - \bar{e})/\sigma_e$, l represents the standardized latitude, and e represents elevation, and finally, $x_3 = x_1 x_2$ is an interaction effect of the covariates.

TABLE 2 Summary statistics for 100 replicates to the proposed model

$n = 400$	$p = 0.80$			$p = 0.95$			$p = 0.99$		
	APM	AMSE	CPI	APM	AMSE	CPI	APM	AMSE	CPI
$\beta_{p,0}$	300.0	0.327	0.92	300.1	0.457	0.98	299.9	1.112	0.92
$\beta_{p,1}$	1.97	0.272	0.89	1.93	0.424	0.93	1.95	0.417	0.92
$\beta_{p,2}$	−2.02	0.181	0.94	−1.97	0.206	0.97	−2.09	0.326	0.92
ν_0	−0.20	0.002	0.91	−0.21	0.002	0.93	−0.20	0.001	0.83
ν_1	−0.10	0.003	0.92	−0.10	0.001	0.96	−0.10	<0.001	0.91
ν_2	0.28	0.001	0.95	0.30	0.001	0.97	0.30	<0.001	0.85
α_0	2.00	0.001	0.94	2.00	0.002	0.93	1.99	0.002	0.92
α_1	−0.10	0.003	0.92	−0.10	0.003	0.92	−0.10	0.001	0.94
α_2	0.20	0.002	0.87	0.21	0.001	0.95	0.20	0.002	0.85
n=1,000	p=0.80			p=0.95			p=0.99		
	APM	AMSE	CPI	APM	AMSE	CPI	APM	AMSE	CPI
$\beta_{p,0}$	300.0	0.130	0.97	300.0	0.150	0.97	300.2	0.519	0.85
$\beta_{p,1}$	1.99	0.111	0.98	1.93	0.122	0.94	1.97	0.172	0.90
$\beta_{p,2}$	−2.01	0.056	0.94	−2.00	0.067	0.97	−2.05	0.115	0.88
ν_0	−0.20	<0.001	0.92	−0.20	<0.001	0.93	−0.19	0.001	0.54
ν_1	−0.10	0.001	0.95	−0.10	<0.001	0.92	−0.10	<0.001	0.85
ν_2	0.30	<0.001	0.91	0.30	<0.001	0.92	0.30	<0.001	0.62
α_0	2.00	<0.001	0.93	2.00	<0.001	0.97	1.99	0.001	0.82
α_1	−0.10	0.001	0.94	−0.10	<0.001	0.92	−0.09	<0.001	0.87
α_2	0.20	<0.001	0.96	0.20	<0.001	0.95	0.18	0.002	0.59
n=2,000	p=0.80			p=0.95			p=0.99		
	APM	AMSE	CPI	APM	AMSE	CPI	APM	AMSE	CPI
$\beta_{p,0}$	300.0	0.327	0.92	300.1	0.457	0.98	300.2	0.206	0.87
$\beta_{p,1}$	1.97	0.272	0.89	1.93	0.424	0.93	1.99	0.092	0.88
$\beta_{p,2}$	−2.02	0.181	0.94	−0.97	0.206	0.97	−2.03	0.044	0.91
ν_0	−0.20	0.002	0.91	−0.21	0.002	0.93	−0.19	<0.001	0.54
ν_1	−0.10	0.003	0.92	−0.10	0.001	0.96	−0.10	<0.001	0.86
ν_2	0.28	0.001	0.95	0.30	0.001	0.97	0.30	<0.001	0.66
α_0	2.00	0.001	0.94	2.00	0.002	0.93	1.99	<0.001	0.78
α_1	−0.10	0.003	0.92	−0.10	0.003	0.92	−0.10	<0.001	0.83
α_2	0.20	0.002	0.87	0.21	0.001	0.95	0.19	0.001	0.59
n=5,000	p=0.80			p=0.95			p=0.99		
	APM	AMSE	CPI	APM	AMSE	CPI	APM	AMSE	CPI
$\beta_{p,0}$	300.0	0.327	0.92	300.1	0.457	0.98	300.4	0.398	0.52
$\beta_{p,1}$	1.97	0.272	0.89	1.93	0.424	0.93	2.01	0.034	0.92
$\beta_{p,2}$	−2.02	0.181	0.94	−0.97	0.206	0.97	−2.10	0.035	0.82
ν_0	−0.20	0.002	0.91	−0.21	0.002	0.93	−0.17	0.002	0.14
ν_1	−0.10	0.003	0.92	−0.10	0.001	0.96	−0.10	<0.001	0.50
ν_2	0.28	0.001	0.95	0.30	0.001	0.97	0.29	<0.001	0.18
α_0	2.00	0.001	0.94	2.00	0.002	0.93	1.98	0.001	0.38
α_1	−0.10	0.003	0.92	−0.10	0.003	0.92	−0.08	0.001	0.34
α_2	0.20	0.002	0.87	0.21	0.001	0.95	0.15	0.004	0.16

Note. APM = the average of posterior means; AMSE = the average of the mean standard error; CPI = the coverage probability of 95% of the credibility intervals.

Table 3 shows the confidence interval for the parameters of the models in the $p = (0.80, 0.95, 0.99)$ quantiles. We observe that the quantile intercept increases as p increases. We can also see that, for all the quantiles, the effect of latitude is significant and negative: The greater latitude, the lower the quantile. When p increases, the negative effect of latitude in the quantile increases. Altitude also has a significant effect on the quantiles, and the magnitude of the effect seems to be similarly independent of the p value. Only for the quantile $p = 0.80$ is there a significant effect of the interaction between altitude and latitude. Regarding the parameters involving σ and ξ, there is a significant effect of latitude and elevation, whereas there is no interaction between these two covariates. In addition, we see that the effect of the covariates on these two parameters is the similarly independent of p. For the value of σ, we have a negative effect for latitude, showing that cities with higher latitudes also have a lower range of temperatures. For altitude, there is only a positive effect for $p = 0.80$, showing that higher altitudes increase the range for the estimation of this quantile. For $p = 0.95$ and $p = 0.99$, altitude

TABLE 3 USA: summary of the estimation results for the proposed model

$p = 0.8$			
$\beta_{0.8,0}$	$\beta_{0.8,1}$	$\beta_{0.8,2}$	$\beta_{0.8,3}$
91.16 (90.72; 91.59)	−3.81 (−4.25; −3.33)	4.25 (3.59; 4.92)	−1.82 (−2.55; −1.04)
ν_0	ν_1	ν_2	ν_3
1.49 (1.44; 1.53)	−0.09 (−0.14; −0.05)	0.11 (0.07; 0.15)	−0.01 (−0.07; 0.03)
α_0	α_1	α_2	α_3
−0.15 (−0.18; −0.11)	−0.12 (−0.15; −0.09)	0.25 (0.23; 0.27)	−0.01 (−0.04; 0.02)
p=0.95			
$\beta_{0.95,0}$	$\beta_{0.95,1}$	$\beta_{0.95,2}$	$\beta_{0.95,3}$
95.14 (94.58; 95.73)	−4.65 (−5.20; −4.01)	4.40 (3.57; 5.43)	−1.06 (−2.16; 0.18)
ν_0	ν_1	ν_2	ν_3
1.42 (1.38; 1.47)	−0.08 (−0.13; −0.03)	−0.02 (−0.06; 0.04)	0.05 (−0.03; 0.11)
α_0	α_1	α_2	α_3
−0.17 (−0.21; −0.14)	−0.10 (−0.13; −0.07)	0.17 (0.16; 0.19)	0.00 (−0.02; 0.02)
p=0.99			
$\beta_{0.99,0}$	$\beta_{0.99,1}$	$\beta_{0.99,2}$	$\beta_{0.99,3}$
98.67 (97.89; 99.53)	−5.70 (−6.37; −5.02)	5.08 (3.99; 6.09)	−1.02 (−2.11; 0.17)
ν_0	ν_1	ν_2	ν_3
1.41 (1.36; 1.45)	−0.09 (−0.14; −0.03)	−0.05 (−0.10; 0.01)	0.05 (−0.01; 0.11)
α_ξ	α_ξ	α_ξ	α_3
−0.18 (−0.21; −0.15)	−0.08 (−0.10; −0.06)	0.13 (0.12; 0.15)	0.00 (−0.02; 0.01)

Note. Posterior means, with 95% credibility intervals, are in parentheses.

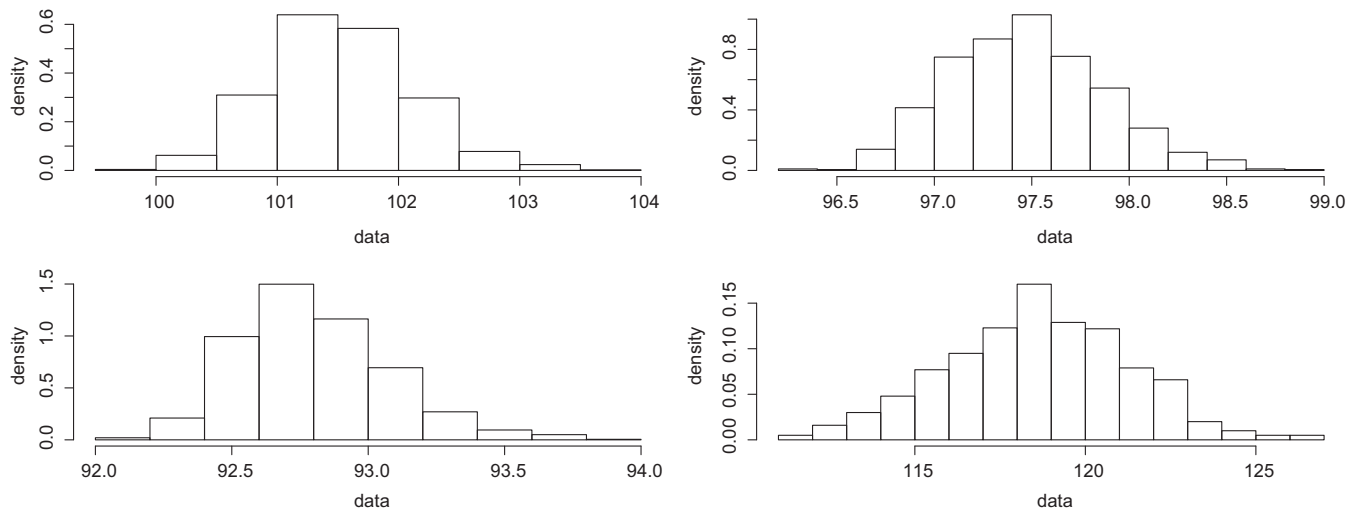

FIGURE 3 Histogram of $q(0.95)$ distribution. (Top) Birmingham, AL (left), and Paducah, KY (right). (Bottom) Flint, MI (left), and Albuquerque, NM (right)

does not seem to influence the σ parameter. For the shape parameter ξ, we find a negative effect on latitude, showing that heavy tails occur in cities with lower latitudes. For altitude, the effect is the opposite, showing that cities with higher altitudes have heavier tails.

Figure 3 shows the histogram of the posterior distribution of the quantile $q(0.99)$ in four cities analyzed by the model, namely, Birmingham, AL (lat=33.39, elev=140 m); Paducah, KY (lat=37.04,elev=115 m); Flint, MI (lat=43.02,elev=260 m); and Albuquerque, NM (lat=35.04, elev=1562 m). The 99% quantile represents the return level expected in every $t = 100$ periods. The figure shows that a temperature of 101.5°F is expected once every 100 years in Birmingham, AL, whereas for Flint, MI, the maximum temperature expected to occur once every 100 years is 92.7°F.

Figure 4 shows the histogram of the same four cities for the distribution of $Q_{0.80}$, which is a more likely event because this quantile is the expected return level every $t = 5$ years. Every five years, the temperature in Paducah, KY, is expected to be greater than 89.8°F at least once, whereas in Albuquerque, NM, this value is 109°F.

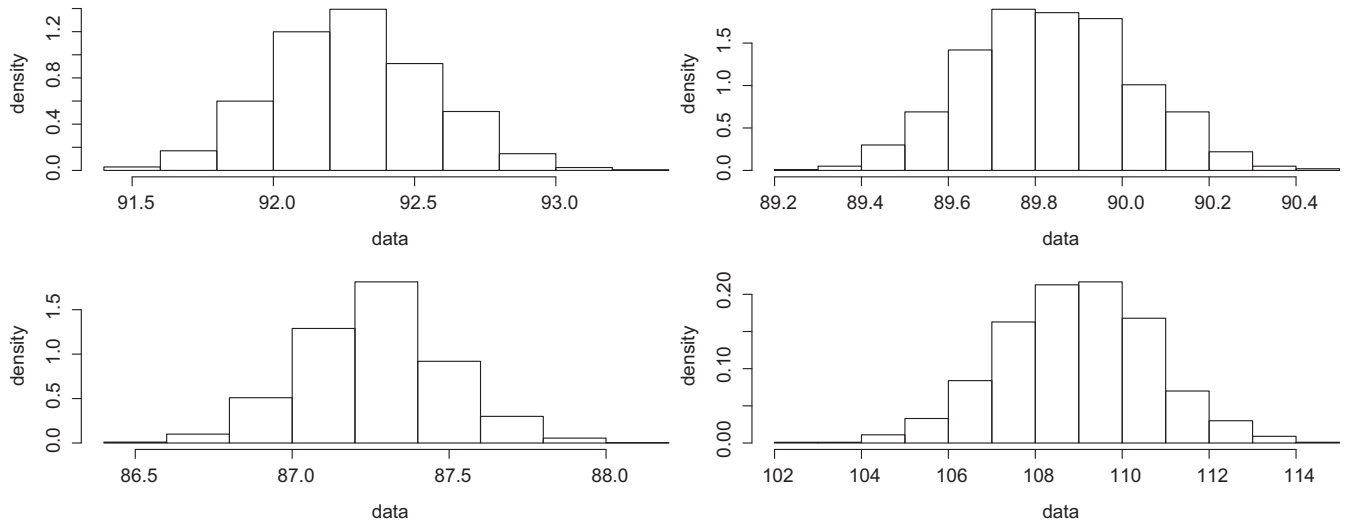

FIGURE 4 Histogram of $q(0.80)$ distribution. (Top) Birmingham, AL (left), and Paducah, KY (right). (Bottom) Flint, MI (left), and Albuquerque, NM (right)

4.2 | Maxima quota of Gurgueia River

The second application represents the monthly maxima river quota in Gurgueia River in Piauí State, northeastern Brazil. A river quota is the height of the water in the section based on a given reference. Conventionally, the quotas are measured in centimeters. Monthly data were collected from 1975 to 2014. In this application, as we have just one station, we do not use the location as the covariates. Instead, we use the season as the covariates, where $x = (x_0, x_1, x_2)$. Here, $x_0 = 1$ is the intercept, $x_1 = \cos(2\pi m/12)$, and $x_2 = \sin(2\pi m/12)$, where m is the month of the observation. The data were collected from 1975 to 2012.

Table 4 shows the parameter estimates of the proposed model. There is a difference of about 105 cm between the intercepts of $q(0.95)$ and $q(0.99)$. Furthermore, the trigonometric movement also shows differences between quantiles. While the covariate x_2 has a stronger weight in the composition of this quantile for $q(0.95)$, the covariate x_1 has a higher parameter value for $q(0.99)$. Regarding ξ and σ, the parameters of the models with $q(0.95)$ and $q(0.99)$ are close, indicating that the quantile used in the model does not influence the values of these parameters. Figure 5 shows this difference in behavior or trigonometric movements.

Figure 5 shows the monthly variation of the quantiles. The extreme quantiles have higher quotas in the initial and final months of the year, which correspond to the rainy season in the state, whereas the high quantiles of the quotas decrease in the middle of the year. For $q(0.95)$, the highest quota corresponds to February (581 cm) and the lowest quota occurs in August (208 cm). For $q(0.99)$, the highest quota occurs in January (715 cm) and the lowest quota occurs in July (285 cm). The right part of Figure 5 shows the time series data with estimates of the high quantiles. The quantiles can adequately capture the behavior of the high quantiles. In 12 of the 415 observations (2.9%), the observed series exceed the estimated $q(0.95)$, whereas in four observations (0.96%), the series exceed $q(0.99)$.

TABLE 4 Gurgueia: summary of the estimation results for the proposed model

p=0.95			p=0.99		
$\beta_{0.95,0}$	$\beta_{0.95,1}$	$\beta_{0.95,2}$	$\beta_{0.99,0}$	$\beta_{0.99,1}$	$\beta_{0.99,2}$
395.1 (365.9; 423.5)	110.5 (68.4; 142.2)	151.6 (125.9; 177.4)	500.7 (465.9; 536.4)	167.3 (139.8; 193.7)	138.7 (113.2; 165.3)
ν_0	ν_1	ν_2	ν_0	ν_1	ν_2
4.12 (4.05; 4.21)	0.21 (0.11; 0.30)	0.51 (0.40; 0.63)	4.07 (4.00; 4.13)	0.23 (0.13; 0.30)	0.56 (0.45; 0.70)
α_0	α_1	α_2	α_0	α_1	α_2
−0.01 (−0.10; 0.07)	0.11 (−0.03; 0.18)	−0.25 (−0.31; −0.15)	0.01 (−0.04; 0.05)	0.08 (0.05; 0.13)	−0.21 (−0.25; −0.18)

Note. Posterior means, with 95% credibility intervals, are in parentheses.

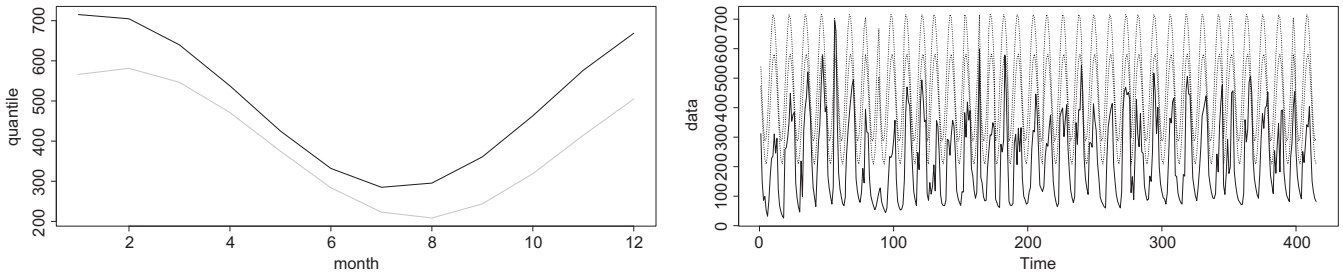

FIGURE 5 Gurgueia River quantile estimation. (Left) Posterior mean of $q(0.95)$ (grey) and $q(0.99)$ black from January to December. (Right) Time series of observations (black) with posterior mean of v and $q(0.99)$ (dotted lines)

4.3 | Maximum temperature in Piauí State

The third data set consists of the monthly maxima temperature (degrees Celsius) from 1961 to 2012 in two cities in the state of Piauí: Picos and Teresina. In this application, we consider the time-varying regression parameters and $x_1 = \cos(2\pi m/12)$ and $x_2 = \sin(2\pi m/12)$, where m is the month, controlling for the seasonal component.

Figure 6 shows the time-varying parameters in Picos. The parameters here vary over time. With respect to the intercept, we see a temporal variation, where $\beta_{0,p}$ has high values as p rises. $\beta_{1,p}$ increases over time in the quantile $p = 0.99$, with a slight decrease for the quantiles $p = 0.95$ and $p = 0.80$. The $\beta_{2,p}$ value is always greater for $p = 0.80$ and has similar values and time variation for $p = 0.95$ and $p = 0.99$.

Figure 7 shows the time-varying parameters in Teresina. For the quantile $p = 0.80$, $\beta_{0,p}$ varies little over time. Furthermore, in the latter observations, $\beta_{0,0.95}$ increases rapidly and exceeds $\beta_{0,0.99}$. For $\beta_{1,0.95}$, the opposite occurs, showing a considerable decay over time. Although there is crossing of lines in some situations where $\beta_{j,p} > \beta_{j,p^*}$ for $p < p^*$, this does not necessarily mean that the quantile p is greater than p^* because the quantile calculation also depends on the linear combination of the variables as described in Equation (8). Figure 8 shows that this change in parameters should decrease the distance between the quantiles p and p^* across the time.

Figure 8 shows the original series of the two cities in addition to the estimation of the high quantiles. The proposed model, with parameters varying over time, captures the behavior of the data efficiently and the high quantiles vary in a similar way to in the original data series.

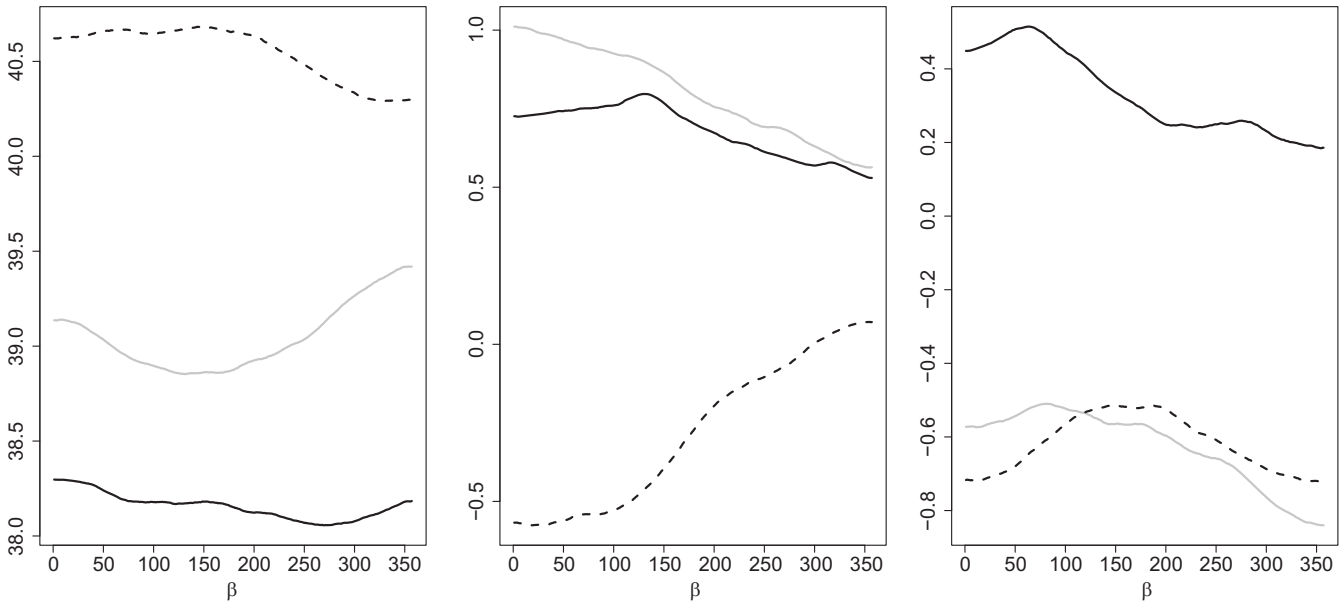

FIGURE 6 Posterior mean of $\beta_{k,p}$ varying in time in Picos. (Left) $\beta_{0,p}$. (Center) $\beta_{1,p}$. (Right) $\beta_{2,p}$. (Black line) $p = 0.80$. (Grey line) $p = 0.95$. (Dotted line) $p = 0.99$

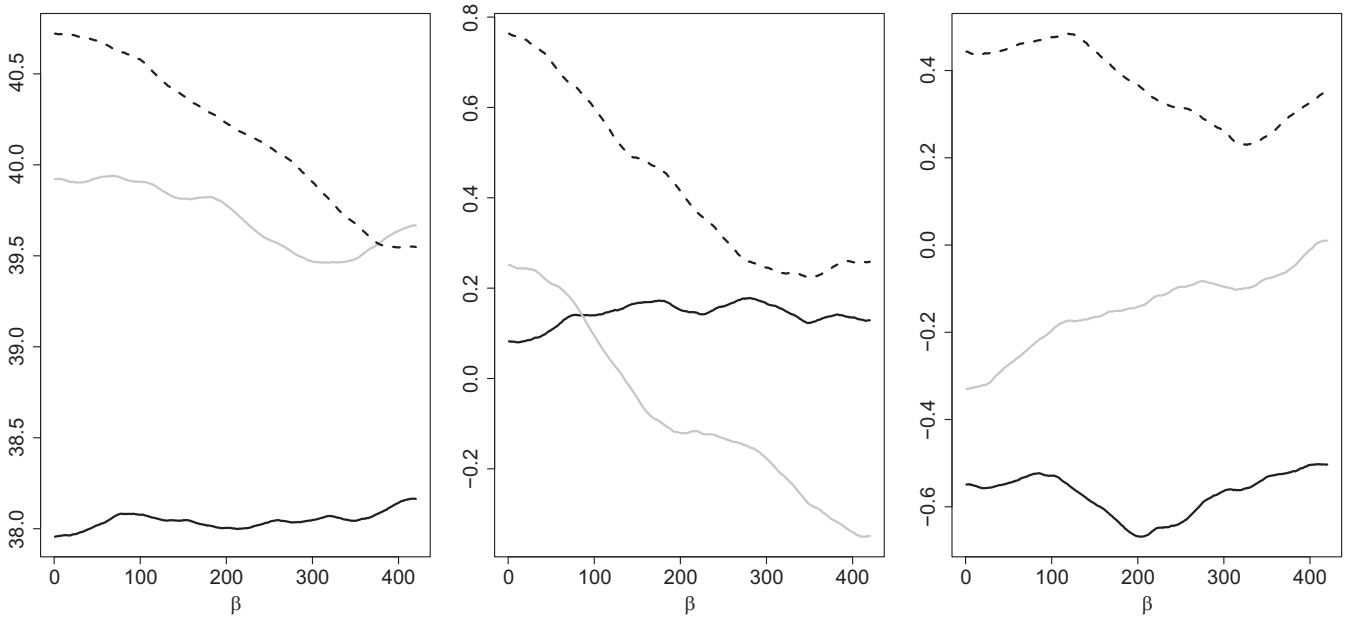

FIGURE 7 Posterior mean of $\beta_{k,p}$ varying in time in Teresina. (Left) $\beta_{0,p}$. (Center) $\beta_{1,p}$. (Right) $\beta_{2,p}$. (Black line) $p = 0.80$. (Grey line) $p = 0.95$. (Dotted line) $p = 0.99$

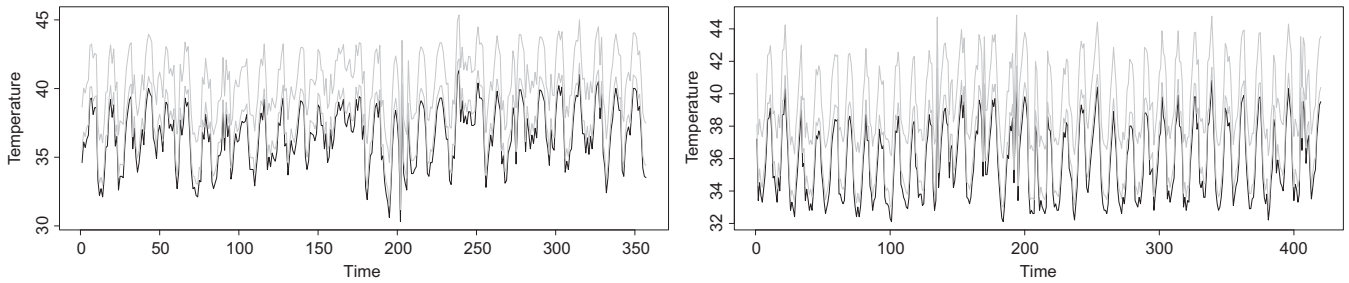

FIGURE 8 Data series (black line) with posterior mean of $q(0.80)$ e $q(0.99)$ (grey line)

5 | CONCLUDING REMARKS

The estimation of high quantiles serves as the main measure when studying extreme values, and this work presented a direct way of obtaining these measurements through reparametrization as a function of the high quantiles. The quantile regression model was also interpretive for any percentile values, indicating which covariates influence the extreme temperature and river quota measurements. We also presented the situation in which the observations vary over time by proposing a dynamic quantile regression model. An application to temperature data showed that the effect on the covariates may differ as time passes. Quantile regression for maxima can be extended to other applications of GEV models, such as generalizations of the GEV distribution (Nascimento, Bourguignon, & Leão, 2016), change point analysis (Nascimento & Silva, 2017), and *r*-largest-order statistics distributions (Silva & Nascimento, 2019).

ORCID

Marcelo Bourguignon https://orcid.org/0000-0002-1182-5193

REFERENCES

Cabras, S., Castellanos, M. E., & Gamerman, D. (2011). A default Bayesian approach for regression on extremes. *Statistical Modelling*, *11*, 557–580.

Coles, S. G. (2001). *An introduction to statistical modelling of extreme values*. London, UK: Springer.

Embrechts, P., Klüppelberg, C., & Mikosch, T. (1997). *Modelling extremal events for insurance and finance*. New York, NY: Springer.

Fisher, R. A., & Tippett, L. H. C. (1928). Limiting forms of the frequency distribution of the largest or smallest member of a sample. *Mathematical Proceedings of the Cambridge Philosophical Society*, *24*, 180–190.

Gaetan, C., & Grigoletto, M. (2004). Smoothing sample extremes with dynamic models. *Extremes*, *7*(3), 221–236.

Gamerman, D., & Lopes, H. F. (2006). *Markov chain Monte Carlo: Stochastic simulation for Bayesian inference* (2nd ed.). Baton Rouge, LA: Chapman and Hall/CRC.

Gonçalves, K., Migon, H. S., & Bastos, L. S. (2018). Dynamic quantile linear model: A Bayesian approach. *Bayesian Analysis*. To appear. https://projecteuclid.org/euclid.ba/1556244057

Huerta, G., & Sansó, B. (2007). Time-varying models for extreme values. *Environmental and Ecological Statistics*, *14*(3), 285–299.

Jenkinson, A. F. (1955). The frequency distribution of the annual maximum (or minimum) values of meteorological events. *Quarterly Journal of the Royal Meteorological Society*, *81*, 158–171.

Kozumi, H., & Kobayashi, G. (2011). Gibbs sampling methods for Bayesian quantile regression. *Journal of Statistical Computation and Simulation*, *81*(11), 1565–1578.

Lima, S., Nascimento, F. F., & Ferraz, V. R. S. (2018). Regression models for time-varying extremes. *Journal of Statistical Computation and Simulation*, *88*(2), 235–249.

Nascimento, F. F., Bourguignon, M., & Leão, J. (2016). Extended generalized extreme value distribution with applications in environmental data. *Hacettepe Journal of Mathematics and Statistics*, *45*(6), 1847–1864.

Nascimento, F. F., Gamerman, D., & Lopes, H. F. (2011). Regression models for exceedance data via the full likelihood. *Environmental and Ecological Statistics*, *18*, 495–512.

Nascimento, F. F., Gamerman, D., & Lopes, H. F. (2016). Time-varying extreme pattern with dynamic models. *TEST*, *25*, 131–149.

Nascimento, F. F, & Silva, W. V. M. (2016). MCMC4Extremes: Posterior distribution of extreme value models in r. Retrieved from https://CRAN.R-project.org/package=MCMC4Extremes

Nascimento, F. F., & Silva, W. V. M. (2017). A Bayesian model for multiple change point to extremes, with application to environmental and financial data. *Journal of Applied Statistics*, *44*, 2410–2426.

Pfaff, B., Zivot, E., McNeil, A., & Stephenson, A. (2018). evir: Extreme values in r. Retrieved from https://CRAN.R-project.org/package=evir

Prado, R., & West, M. (2010). *Time series modeling, computation, and inference*. Boca Raton, FL: Chapman and Hall/CRC.

Silva, R., & Nascimento, F. F. (2019). *Extreme value theory applied to R largest-order statistics under the Bayesian approach*. Revista Colombiana De Estadstica. To appear.

von Mises, R. (1954). La distribution de la plus grande de n valeurs. In Selected Papers, Volume 2 (pp. 271-294). Providence, RI: American Mathematical Society.

West, M., & Harrison, J. (1997). *Bayesian forecasting and dynamic models*. (2nd ed.). New York, NY: Springer.

Yu, K., & Moyeed, R. A. (2001). Bayesian quantile regression. *Statistics & Probability Letters*, *54*(4), 437–447.

How to cite this article: Ferraz Do Nascimento F, Bourguignon M. Bayesian time-varying quantile regression to extremes. *Environmetrics*. 2019;e2596. https://doi.org/10.1002/env.2596